Available online at www.sciencedirect.com
ScienceDirect
Neuromuscular Disorders xxx (xxxx) xxx
www.elsevier.com/locate/nmd

Excitability Properties of Mouse and Human Skeletal Muscle Fibres Compared by Muscle Velocity Recovery Cycles

K.J. Suetterlin[a,b,*], R. Männikkö[a], E. Matthews[a,c], L. Greensmith[a], M.G. Hanna[a], H. Bostock[a], S.V. Tan[a,d]

[a] *Department of Neuromuscular Diseases, UCL Queen Square Institute of Neurology, London, United Kingdom*
[b] *AGE Research Group, NIHR Newcastle Biomedical Research Centre, Newcastle upon Tyne Hospitals NHS Foundation Trust and Newcastle University, Newcastle upon Tyne, United Kingdom*
[c] *Atkinson Morley Neuromuscular Centre, Department of Neurology, St Georges University Hospitals NHS Foundation Trust, London, United Kingdom*
[d] *Department of Neurology and Clinical Neurophysiology, Guy's & St Thomas' NHS Foundation Trust and Institute of Psychiatry, Psychology & Neuroscience, Division of Neuroscience, King's College London, United Kingdom*

Received 11 July 2021; received in revised form 27 January 2022; accepted 22 February 2022
Available online xxx

Abstract

Mouse models of skeletal muscle channelopathies are not phenocopies of human disease. In some cases (e.g. Myotonia Congenita) the phenotype is much more severe, whilst in others (e.g. Hypokalaemic periodic paralysis) rodent physiology is protective. This suggests a species' difference in muscle excitability properties. In humans these can be measured indirectly by the post-impulse changes in conduction velocity, using Muscle Velocity Recovery Cycles (MVRCs). We performed MVRCs in mice and compared their muscle excitability properties with humans. Mouse Tibialis Anterior MVRCs ($n=70$) have only one phase of supernormality (increased conduction velocity), which is smaller in magnitude ($p=9\times10^{-21}$), and shorter in duration ($p=3\times10^{-24}$) than human ($n=26$). This abbreviated supernormality is followed by a period of late subnormality (reduced velocity) in mice, which overlaps in time with the late supernormality seen in human MVRCs. The period of late subnormality suggests increased t-tubule Na^+/K^+-pump activity. The subnormal phase in mice was converted to supernormality by blocking ClC-1 chloride channels, suggesting relatively higher chloride conductance in skeletal muscle. Our findings help explain discrepancies in phenotype between mice and humans with skeletal muscle channelopathies and potentially other neuromuscular disorders. MVRCs are a valuable new tool to compare *in vivo* muscle membrane properties between species and will allow further dissection of the molecular mechanisms regulating muscle excitability.

Keywords: Muscle velocity recovery cycles (MVRCs); Excitability; ClC-1; Skeletal muscle channelopathies; Mouse model; Translational gap.

1. Introduction

Animal models of disease allow exploration of physiological functions and systemic interactions between organs [1]. Mice have become the preferred model of disease, due to their relative ease of genetic manipulation, similarities in biochemistry and physiology and low cost [2]. However, translation of findings from animal models of neuromuscular disease to human patients has been poor [2,3]. Understanding how and why the neuromuscular functions differ between the species will improve the value of the mouse as a model organism and may even indicate potential protective mechanisms that inform novel therapies.

Skeletal muscle channelopathies are rare disorders caused by mutations in genes encoding skeletal muscle ion channels that result in over- or under-excitability of the muscle. The classic skeletal muscle channelopathies present clinically with myotonia or periodic paralysis (PP). Non-dystrophic myotonias are caused by loss-of-function mutations of the skeletal muscle chloride channel ClC-1 or by gain-of-function

* Corresponding author.
E-mail addresses: karen.suetterlin@nhs.net, karen.suetterlin@newcastle.ac.uk (K.J. Suetterlin).

https://doi.org/10.1016/j.nmd.2022.02.011

mutations of the skeletal muscle sodium channel $Na_V1.4$ [4]. Myotonia related to reduced ClC-1 function is also observed in Myotonic Dystrophy type 1 and 2. Periodic paralyses (PP) are caused by gain-of-function mutations in either $Na_V1.4$ or the skeletal muscle calcium channel $Ca_V1.1$, or by loss of function in Kir2.1 [4]. Biallelic loss-of-function mutations in $Na_V1.4$ or $Ca_V1.1$ ion channels have also been reported in association with congenital myopathy [5,6] and congenital myasthenia [7–10].

The species difference in channelopathy presentation is exemplified by mouse models of myotonia congenita (MC) [11,12] and hypokalaemic PP [13,14]. In contrast to humans with recessive MC, who are considered non-dystrophic and believed to have normal lifespan, adr mice with biallelic loss-of-function in chloride channels, as in MC, exhibit reduced life span, low body weight and significant muscle atrophy. This is despite similar reductions in sarcolemmal chloride conductance between adr mice and humans with recessive MC [11,15].

Conversely, whilst spontaneous attacks of weakness are one of the defining clinical features of hypokalaemic PP in humans, the two transgenic mouse models of hypokalaemic PP have locomotor behaviour indistinguishable from controls [13,14]. This apparent resistance to spontaneous paralytic attacks was also observed in an acquired (potassium-deficient) rat model of periodic paralysis [16]. As changes in muscle ion channels show different consequences in mice and humans, we suspected that the intrinsic muscle excitability properties may differ between the species.

To obtain information about muscle membrane potential and ion channels, we have used the recently established method of muscle velocity recovery cycles (MVRCs) [17]. The velocity of muscle action potentials increases during the negative afterpotential following an impulse, and the velocity changes provide a sensitive indication of the resting membrane potential [18]. Single-fibre recordings have demonstrated that such velocity recovery functions (or recovery cycles) can help reveal muscle membrane dysfunction in muscular dystrophy and denervation [19], but the method has proved too technically challenging for clinical use. The use of multi-fibre recordings [17] has overcome this limitation, and multi-fibre MVRCS using 1–5 conditioning stimuli have been validated as a repeatable technique [20,21], that reveals consistent evidence of membrane depolarization in patients with chronic renal failure [22] and critical illness myopathy [23,24], and evidence of dysfunction of specific ion channels in patients with MC [25], sodium channel myotonias [26], Andersen-Tawil syndrome [27] and PP [28].

We have previously shown that MVRC recording is technically feasible in mice and is also sensitive enough to detect changes in muscle excitability properties due to genetic ion channel dysfunction [29]. Here we compare MVRCs recorded *in vivo* from human and mouse muscles and describe pharmacological experiments to help account for the marked species differences in intrinsic membrane properties. These differences may help explain some of the differences in channelopathy presentation described above.

2. Methods

2.1. Animals

C57/BL J6 mice were used: 34 recordings were from male tibialis anterior (TA) muscle and 36 recordings were from female TA. The mean age of animal was 28 ± 16.2 weeks, and the range was 13 to 77 weeks. We have previously shown that mouse TA MVRCs with up to 5 conditioning stimuli do not change significantly with age [29]. Mice were fed *ad libitum* and housed according to home office guidelines. Experiments were carried out under licence from the UK Home Office (Scientific Procedures Act 1986) and following approval by the UCL Institute of Neurology Animal Welfare Ethical Review Panel.

2.2. Healthy human volunteers

Human recordings were performed on the TA of 10 healthy male volunteers (age 48 ± 12 years) and 16 healthy female volunteers (age 42 ± 13 years) as previously described [25,27,30]. Informed written consent was obtained from all subjects according to the Declaration of Helsinki. The study was approved by St Thomas Hospital, London, UK and University College London research ethics committees (10/H0802/6).

2.3. Mouse muscle velocity recovery cycle (MVRC) recording in vivo

In contrast to humans, an anaesthetic is required to perform MVRCs in mice. For the first few recordings, when developing the MVRC technique, chloral hydrate was used and administered via intraperitoneal injection. However, we changed to inhaled anaesthesia as this can be adjusted and maintained without requiring additional intraperitoneal injection, which on occasion disturbed the recording electrodes. Inhalational anaesthetics have been shown to modulate Na_V channels *in vitro* and isoflurane is known to reduce cortical excitability [31]. There is no such report for chloral hydrate. There was no apparent difference in the morphology or parameters of the initial mouse MVRCs recorded using intraperitoneal chloral hydrate and the subsequent MVRCs recording using inhaled isoflurane anaesthesia. This is in keeping with the finding that there was no difference in mouse peripheral nerve excitability measurements recorded under the influence of inhaled isoflurane or intraperitoneal injection of chloral hydrate [32] and the finding that sevoflurane had no effect on the recovery cycle of human corticospinal axons [33].

After induction, the mouse was placed on its back on a heat mat and anaesthesia maintained via a nose cone (Fig. 1). MVRCs were performed as described previously

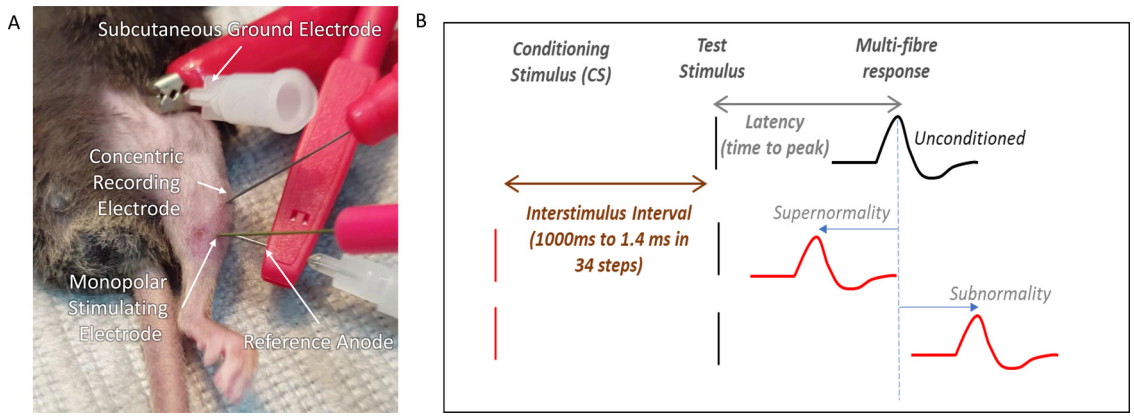

Fig. 1. Experimental setup for MVRCs in mouse TA muscle. A monopolar stimulating needle electrode (28 G TECA, Viasys Healthcare Madison, Wisconsin) was inserted into the distal muscle. A reference anode was inserted above the monopolar stimulating electrode on the lateral edge of the muscle. The reference anode consisted of a 27 G hollow bore disposable steel needle attached to reference anode lead with crocodile clip. Stimuli consisting of 0.05 ms rectangular current pulses were delivered. Muscle activity was recorded with a concentric needle electrode (disposable 30 G concentric EMG needle, TECA) inserted into the proximal end of the muscle. A ground electrode was inserted under the skin in the axilla. The ground electrode consisted of a 27 G hollow bore disposable steel needle that was bent to make it easier to insert under the skin and attached to crocodile clip on the ground cable. B. A schematic of the stimulation and recording protocol with one conditioning stimulus is shown. Latencies are measured from the test stimulus to the peak of the multifibre response. The response to the test stimulus alone is referred to as an unconditioned response. The response to a test stimulus preceded by one or more conditioning stimuli is referred to as a conditioned response. The time interval between conditioning and test stimuli is known as the Interstimulus Interval (ISI) and is varied (34 different time intervals between 1.4 and 1000 ms). A reduction in the latency of the conditioned response relative to the latency of the unconditioned response is referred to as supernormality, and an increase in latency as subnormality. The latency of the conditioned response is expressed as a percentage change compared to the latency of the unconditioned response and plotted for the range of ISIs up to 1000 ms (see Fig. 2).

[29]. A bundle of fibres in the muscle was excited via a monopolar needle, and the multifibre response was recorded more proximally via a concentric needle electrode. The electrode positions were adjusted to obtain a stable negative peak response with a current stimulus of 3–10 mA. The response was amplified at a gain of 1000, filtered with bandwidth 50 Hz to 2 kHz and digitised (NI DAQ) using a sampling rate of 20 kHz. Stimulation and recording were controlled by QTRACW software (© UCL Queen Square Institute of Neurology, London) using the M3REC3.QRP protocol. Surface temperature over the muscle was recorded at the end of the recording using an infra-red thermometer. MVRCs were recorded with 1, 2 and 5 conditioning stimuli, all separated by 10 ms intervals. Test stimuli were delivered every 2 s. The inter-stimulus interval (ISI) between the last conditioning stimulus and the test stimulus varied from 1000 to 1.4 ms in 34 steps in an approximately geometric series (specifically 1000, 900, 800, 700, 600, 500, 450, 400, 350, 300, 260, 220, 180, 140, 110, 89, 71, 56, 45, 35, 28, 22, 18, 14, 11, 8.9, 7.1, 5.6, 4.5, 3.5, 2.8, 2.2 and 1.8 ms, Fig. 1B) [17,25].

A conditioned stimulus refers to a test stimulus preceded by either 1, 2 or 5 conditioning stimuli at one of the 34 different interstimulus intervals. An unconditioned stimulus refers to a test stimulus alone (Fig. 1B). The time from test stimulus to the peak of compound muscle action potential response is always measured and referred to as latency. The latency change compares response to a conditioned test stimulus with response to an unconditioned test stimulus at each of the 34 different interstimulus intervals. A reduction in latency (increased conduction velocity) is known as supernormality. An increase in latency (decreased conduction velocity) is known as subnormality (Fig. 1B).

2.4. MVRCs with CLC-1 inhibition

Baseline MVRCs were performed (as described above). Afterwards intraperitoneal injection of 9 anthracene carboxylic acid (9AC) was administered with MVRC recording electrodes still *in situ*. The dose of 9AC used was either 5 mg/kg or 30 mg/kg (as described for an *in vivo* rat model of myotonia [34]). A minimum of 10 min after injection, MVRCs were repeated on the same TA before being performed on the contralateral TA. For this reason, when all recordings were successful there could be more recordings post injection than pre injection from the same animal. All recordings were completed within 60 min of 9AC administration.

2.5. Statistical analysis

To determine statistical significance Welch or Welch rank test was performed depending on normality (Liliefor's test). As multiple parameters were compared an increased threshold for statistical significance of $p \leq 0.01$ was applied.

3. Results

3.1. Muscle velocity recovery cycles (MVRCs)

Human MVRCs have two phases of supernormality (Fig. 2A). The first peaks before an interstimulus interval (ISI) of 15 ms (Table 1, Fig. 2A, purple bracket). This is

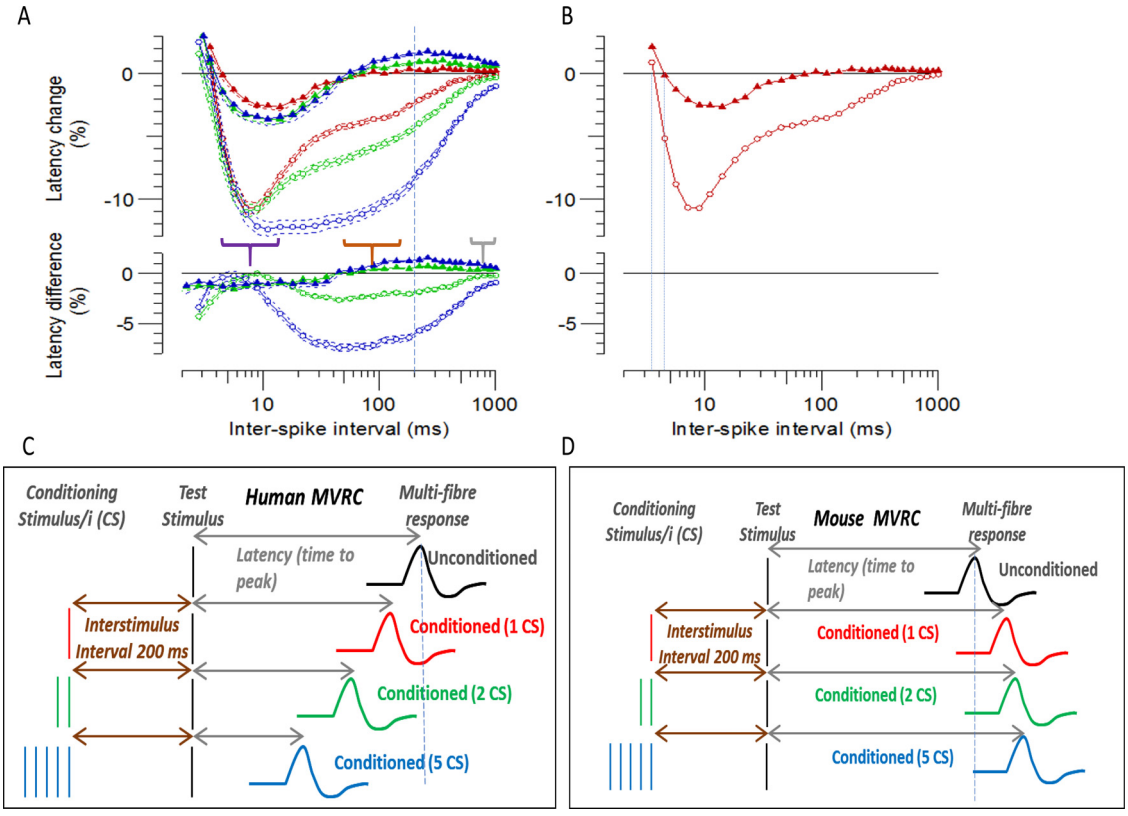

Fig. 2. Comparison of MVRCs from humans and mice. A. Comparison of MVRCs in response to 1 (red), 2 (green) and 5 (blue) conditioning stimuli from humans ($n=26$, open circles) and mouse TA ($n=70$, filled triangles). The purple bracket delineates the period of early supernormality (<15 ms ISI), the orange bracket the period of late supernormality (50–150 ms ISI) and the grey bracket residual supernormality (900–1000 ms ISI). The dashed line marks the interstimulus interval of 200 ms referred to by the schematic in C and D B. Data is the same as in A but limited to MVRCs in response to 1 conditioning stimulus to demonstrate the increased Muscle Relative Refractory Period (MRRP) in mouse compared to human TA. MRRP is the point at which the latency change between conditioned and unconditioned stimuli is 0% and represents the end of the relative refractory period of the excitability recovery cycle. The dashed line marks the interstimulus interval corresponding to the MRRP. C & D. A schematic showing the relative latencies (measured to peak) at an ISI of 200 ms, for test stimulus (0.05 ms current pulses) given alone and with 1, 2 or 5 equal conditioning stimuli in human muscle (C), and mouse muscle (D). At an interstimulus interval of 200 ms (dashed line in A), the conditioned latencies are reduced in human muscle (C) but increased in mouse muscle (D). Data are mean±SEM.

Table 1
Human and Mouse Muscle Velocity Recovery Cycle Measurements (MVRCs) compared using parameters described for human MVRCs.

Excitability Measures	Mean ± SEM (n)		P for Welch rank test (non-parametric)
	Human TA	Mouse TA	Human Vs Mouse
MRRP	3.70±0.12 (26)	4.79±0.23 (67)	$p=0.00128$*
ESN (%)	11.19±0.44 (26)	3.33±0.29 (67)	$p=9.21\times10^{-21}$*
ESN@(ms)	7.98±0.23 (26)	10.78±0.36 (67)	$p=7.08\times10^{-9}$*
SNEnd (ms)	745.3±39.5 (26)	53.55±5.12(66)	$p=6.97\times10^{-23}$*
5ESN (%)	13.01±0.54 (26)	4.90±0.51 (62)	$p=1.21\times10^{-15}$*
LSN (%)	3.68±0.17 (26)	0.013±0.066 (70)	$p=2.61\times10^{-24}$*
2XLSN (%)	2.25±0.15 (26)	−0.323±0.075 (70)	$p=3.12^{-}\times\ 10^{23}$*
5XLSN (%)	7.03±0.31 (26)	−0.83±0.15 (70)	$p=2.62\times10^{-24}$*
RSN (%)	0.125±0.037 (26)	−0.248±0.044 (68)	$p=8.90\times10^{-9}$*
5XRSN (%)	0.986±0.081 (26)	−0.568±0.068 (68)	$p=1.15\times10^{-21}$*

TA, Tibialis Anterior; MRRP, muscle relative refractory period; ESN, early supernormality (up to 15 ms); ESN@, interstimulus interval for maximum ESN; SNEnd, time supernormal period to 1 conditioning stimulus ends, 5ESN, early supernormality after 5 conditioning stimuli; LSN, late supernormality (50–150 ms); 2XLSN extra supernormality after 2 conditioning stimuli compared with 1 conditioning stimulus; 5XLSN, extra supernormality after 5 conditioning stimuli compared with 1 conditioning stimulus; RSN, residual supernormality (900–1000 ms); 5XRSN, extra residual supernormality after 5 conditioning stimuli. *$p<0.01$.

referred to as 'early supernormality' (ESN) [17] and has been proposed to reflect the effect of the depolarising afterpotential. The second phase, which typically increases in magnitude with larger numbers of conditioning stimuli (Fig. 2A), has been proposed to reflect the depolarising effect of potassium accumulation in the t-tubules, and is referred to as 'late supernormality '(LSN) because it is usually maximal at an ISI of 50 to 150 ms [17] (Fig. 2A orange bracket, Table 1). The late supernormality gradually declines over about 1 s, although in response to 5 conditioning stimuli there is usually some residual supernormality (RSN) in human MVRCs at an inter-stimulus interval of 1000 ms (Fig. 2A grey bracket, Table 1) [25].

The morphology of mouse MVRCs showed clear differences from human recordings (Fig. 2, Table 1). Firstly, mouse MVRCs have only one phase of supernormality. This single phase of supernormality is smaller (ESN mouse $3.33 \pm 0.29\%$ vs human $11.19 \pm 0.44\%$, $p = 9.2 \times 10^{-21}$) and peaks later (10.78 ms ± 0.36 mouse vs 7.98 ms ± 0.23 human, $p = 7.1 \times 10^{-9}$) than the first phase of supernormality in human MVRCs and ends at an inter-stimulus interval of about 50 ms (mean 53.6 ± 5.1), equivalent in timing to the early part of the late supernormal period in humans (Fig. 2A). Secondly, this single period of supernormality in mouse MVRCs is followed by a period of late *sub*normality that gradually reduces towards baseline at an ISI of about 1000 ms (Fig. 2A, Table 1). Late subnormality has not been reported for human or pig MVRCs [17,35,36]. Thirdly, in mice, increasing the number of conditioning stimuli has a small and uniform effect across the MVRC whilst in humans, increasing the number of conditioning stimuli has a larger and more disproportionate effect on late supernormality (Fig. 2A). Furthermore, in contrast to the increase in magnitude of the late supernormality seen in humans [17,35,36], increasing the number of conditioning stimuli increased the degree of late *sub*normality in mouse, i.e. 5 conditioning stimuli resulted in both increased supernormality and increased late subnormality in mice (Fig. 2A, Table 1). Finally, the muscle relative refractory period (MRRP) (time interval at which there is no difference between a conditioned and unconditioned stimulus) was significantly longer in mouse TA compared to human TA MVRCs (Fig. 2B, Table 1. $p = 0.001$).

3.2. MVRCs with CLC-1 inhibition

A dose of 5 mg/kg intraperitoneal 9AC was sufficient to induce clinical and electrical myotonia (Fig. 3A). This was evident by approximately 6 min post injection. MVRCs performed at least 10 min after intraperitoneal injection of 5 mg/kg 9AC appeared to increase the amplitude and duration of supernormality but maintained overall mouse MVRC morphology (i.e., a single phase of supernormality that is followed by subnormality). Moreover, there were no significant differences in MVRC parameters compared to MVRCs from the same animals recorded prior to intraperitoneal injection of 9AC (Fig. 3B & C).

Increasing the dose of 9AC to one established for a rat model of myotonia congenita (30 mg/kg) [34] increased the duration of supernormality to a single stimulus ($p = 0.004$), removed late *sub*normality and induced late *super*normality in mouse TA (Fig. 3D & E, Table 2). The presence of 30 mg/kg 9AC augmented the effect of conditioning stimuli, especially for the late supernormality that was now present (Fig. 3E, Table 2). There was a trend towards a reduced MRRP with 30 mg/kg 9AC but this effect was not statistically significant (Fig. 3, Table 2).

4. Discussion

This study was undertaken to test the hypothesis that there are differences in intrinsic membrane properties between mouse and human skeletal muscle. Our principle finding is clear: MVRCs demonstrate that mouse muscle membrane properties are very different from those in humans, so it is not surprising that the clinical presentations of genetically identical channelopathies also differ between the two species. We review the membrane properties underlying early and late supernormality and how these differ between mice and humans. We then consider possible physiological reasons why these differences may be necessary and the relevance of these differences to the use of mice as models of neuromuscular diseases in general and muscle channelopathies in particular.

4.1. The ionic basis of early and late supernormality

The biophysical basis of early and late supernormality has been discussed in detail [17] As first proposed by Frank for frog muscle [37], the rapid repolarization phase of the action potential ends with the membrane slightly depolarized (since influx of sodium ions exceeds efflux of potassium ions), and this negative afterpotential decays passively. As in myelinated nerve, it results in an increase in excitability and conduction velocity [18,38]. In addition and specific to skeletal muscle (i.e. not seen in nerve), there is also a late afterpotential, first described in frog muscle [39]. The late afterpotential summates with trains of impulses and is associated with potassium accumulation in the t-tubule system [40,41]. The late afterpotential correlates with the late phase of supernormality seen in human MVRCs [17] and, in frog muscle, disappears with de-tubulation [39].

4.2. How do muscle membranes in mice differ from those in humans?

The most striking differences between mouse and human MVRCs are the replacement of impulse-dependant late *super*normality by impulse-dependant late *sub*normality and the reduced effect of conditioning stimuli in mouse muscle. Both observations point to species' differences in the buffering or removal of activity-dependant increases in t-tubule potassium.

In rats and presumably also in mice, the effect of potassium accumulation in the t-tubules is countered by

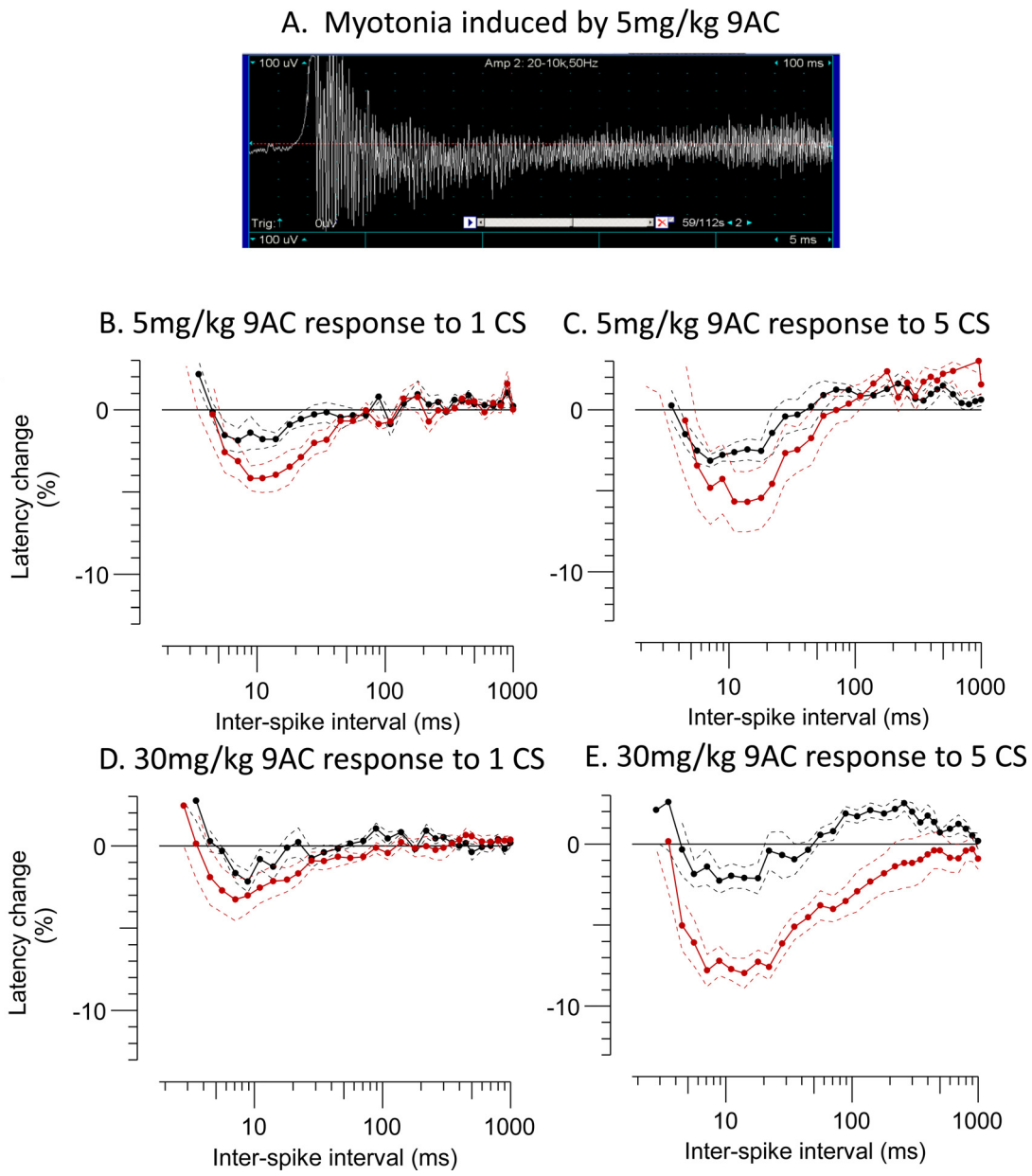

Fig. 3. The effect of 9-Anthracene Carboxylic Acid (9AC) on mouse MVRCs. **A.** Mouse TA EMG recording showing myotonia induced by 5 mg/kg 9AC. **B.** Mouse TA MVRCs in response to 1 conditioning stimulus pre (black, $n=7$) and post (red, $n=6$) 5 mg/kg 9AC. **C.** Mouse TA MVRCs in response to 5 conditioning stimuli pre (black, $n=7$) and post (red, $n=6$) 5 mg/kg 9AC. **D.** Mouse TA MVRCs in response to 1 conditioning stimulus pre (black, $n=4$) and post (red, $n=8$) 30 mg/kg 9AC. **E.** Mouse TA MVRCs in response to 5 CS pre (black, $n=4$) and post (red, $n=8$) 30 mg/kg 9AC. Data are mean±SEM.

the t-system chloride conductance [42]. The observation that healthy human muscle shows marked activity-dependant supernormality, but healthy mouse muscle exhibits this only when the ClC-1 channel is blocked, suggests a relatively larger contribution of ClC-1 current in limiting membrane potential depolarization upon t-tubule potassium accumulation in mice. When we blocked ClC-1 channels with 9AC (Fig. 3), the conduction velocity became sensitive to the number of conditioning stimuli and there was clear late supernormality and even residual supernormality. The effect of ClC-1 blockade on late supernormality also provides indirect evidence of ClC-1 localisation to the t-tubules as the late afterpotential, with which late supernormality correlates, is abolished with de-tubulation [39].

Like our mouse recordings with 9AC, MVRCs from humans with myotonia due to reduced ClC-1 conductance exhibit increased supernormality, with the predominant effect on late and residual supernormality [25]. As in the mice, the sensitivity to conditioning stimuli is also increased in patients with MC, and the increase in late and residual supernormality is most marked in response to 5 conditioning stimuli [25].

We have not found in the literature any direct measurements of both sarcolemmal membrane conductance

Table 2
Mouse TA Muscle Velocity Recovery Cycle Measurements (MVRCs) pre and post 30 mg/kg 9 Anthracene Carboxylic Acid Administration compared using parameters described for human MVRCs.

Excitability Measures	Mean ± SEM (n)		P for Welch rank test (nonparametric)
	Mouse TA Pre 9AC	Mouse TA Post 9AC	Pre Vs post 9AC
MRRP	4.565 ± 0.388(4)	3.568 ± 0.517(6)	$p = 0.18159$
ESN (%)	2.245 ± 0.619(4)	4.736 ± 1.07(7)	$p = 0.09406$
ESN@(ms)	8.45 ± 0.45(4)	8.057 ± 1.25(7)	$p = 0.32082$
SNEnd (ms)	26.32 ± 7.55 (4)	213.2 ± 92.9 (8)	$p = 0.004^*$
5ESN (%)	2.965 ± 0.513(4)	9.003 ± 0.837(8)	$p = 0.0003^*$
LSN (%)	−0.5475 ± 0.0981(4)	0.3513 ± 0.194(8)	$p = 0.0003^*$
2XLSN (%)	−0.205 ± 0.249(4)	0.855 ± 0.785(8)	$p = 0.39552$
5XLSN (%)	−0.8475 ± 0.338(4)	2.964 ± 1.03(8)	$p = 0.00634^*$
RSN (%)	0.07 ± 0.122(4)	−0.34 ± 0.241(7)	$p = 0.12528$
5XRSN (%)	−0.5125 ± 0.351(4)	0.7229 ± 0.726(7)	$p = 0.24414$
Latency(ms)	1.757 ± 0.147(4)	2.041 ± 0.0797(8)	$p = 0.23724$

TA, Tibialis Anterior; MRRP, muscle relative refractory period; ESN, early supernormality (up to 15 ms); ESN@, interstimulus interval for maximum ESN; SNEnd, time supernormal period to 1 conditioning stimulus ends, 5ESN, early supernormality after 5 conditioning stimuli; LSN, late supernormality (50–150 ms); 2XLSN extra supernormality after 2 conditioning stimuli compared with 1 conditioning stimulus; 5XLSN, extra supernormality after 5 conditioning stimuli compared with 1 conditioning stimulus; RSN, residual supernormality (900–1000 ms); 5XRSN, extra residual supernormality after 5 conditioning stimuli. $^*p<0.01$.

and chloride conductance in mice or humans, but in isolated EDL muscles from female Wistar rats the chloride conductance constituted approximately 90% of total resting membrane conductance (1314 ± 72 μS/cm^2, and 1458 ± 70 μS/cm^2 respectively) [43]. In human muscle, combined blockade of chloride and sodium conductance resulted in a 69.3% reduction of resting membrane conductance in human abdominal muscle [44], suggesting that the percentage contribution of chloride conductance to total resting membrane conductance was at least 20% lower in human abdominal muscle compared with rat EDL. In addition, total resting membrane conductance of human abdominal muscle (427 ± 16 μS/cm^2) is only about 30% of that measured in rat EDL. If mouse muscle has similar properties to rat, then it is possible that, not just as a proportion of total resting membrane conductance but also in absolute terms, skeletal muscle chloride conductance may be much larger in mouse than in humans. If this is true, then the late supernormality seen in large mammals might be shorted out by relatively greater t-tubular chloride conductance in rats and mice. Larger total resting conductance (smaller input resistance) may also contribute to the reduced amplitude of supernormality in mouse compared to human muscle (Fig. 2A).

However, it was intriguing that we required such high doses of 9AC - more than that required to trigger myotonia - to see late and residual supernormality in mouse MVRCs. One possible reason for this discrepancy between the presence of clinical myotonia with 5 mg/kg 9AC, but no significant difference on MVRCs with 5 conditioning stimuli is that physiological activation of muscle will involve much longer trains of action potentials than the 5 conditioning stimuli delivered during MVRCs. The fact that there is clinical myotonia with 5 mg/kg 9AC suggests that the dose is sufficient to alter membrane excitability, but, in contrast to humans with MC [25], 5 conditioning stimuli is not sufficient to cause significant change on mouse MVRCs. This may be due to more effective t-tubule potassium reuptake in mouse muscle such that chloride channel blockade must be near complete for the effect of 5 conditioning stimuli on mouse MVRCs to be seen.

Two mechanisms have been described in mouse muscle for the removal of t-tubule potassium: inward rectifier (Kir) potassium currents [45] and potassium reuptake via the alpha-2 isoform of the Na^+/K^+-ATPase sodium pump (α2-pump) [46]. Of these only the α2-pump, with its 3:2 Na^+:K^+ stoichiometry, generates a net hyperpolarizing current while moving potassium intracellularly. For this reason, and because it has been shown to be strongly activated by t-tubule potassium almost immediately following an action potential [46], the α2-pump is the obvious candidate for generating the impulse-dependant late subnormality. The hyperpolarization would then assist further potassium removal by the Kir channels. Targeted knock-out of the skeletal muscle isoform of the α2-pump yields mice that are apparently normal under basal laboratory conditions but show significant impairment on graded treadmill running [47]. Whilst control mice can easily run up to 26 metres/min, the α2-pump knock-out mice were unable to maintain speeds of 4 metres/min [47]. Moreover, at higher treadmill speeds the failure was immediate, before local or systemic factors associated with exercise performance could be inferred [47]. The speed and reversibility of this exercise failure would be consistent with depolarisation-induced weakness secondary to a failure of t-tubule potassium reuptake. Experiments targeting the role of the α2-pump and Kir2.1 channels are required to confirm their contribution to mouse MVRC subnormality. However, currently no *in vivo* dose for selective blockade of either the α2-pump or Kir2.1 channels in skeletal muscle is established. Developing the MVRC technique so it can be performed on isolated muscles *ex vivo* would bypass this technical issue as micromolar ouabain could be used to selectively inhibit

the α2-pump [46] and/or barium to selectively block Kir2.1 channels [45].

4.3. Why should muscle function be different in mice and humans?

Muscle fibres in mice appear structurally similar to those in humans, with diameters of about 50 μm, similar sliding filament contractile apparatus, with resting sarcomere length close to 2.5 μm [48,49], juxtaposed to a similar t-tubule system. The laboratory mouse shares ~99% of its genes with humans and for many years transgenic mice have been used successfully to determine the function of skeletal muscle proteins [50,51]. Yet, when it comes to using mice as models for neuromuscular disease, there are limitations [52–55]. These may in part be due to biomechanical differences in muscle function during walking [54], but the most obvious difference between mice and humans, is that they differ in size and weight by over three orders of magnitude – and the 'physiological clock' of smaller animals ticks faster: smaller animals have shorter lives, they grow up and reproduce more quickly, their hearts beat faster, and their movements are more rapid [56–58].

Animals of similar shape differing by a factor of 1000 in size have muscles that differ little in force per unit area, and differ little in running speed, but the smaller animal has to move its limbs 10 times more rapidly to achieve this [57]. If humans tried to contract TA muscles 10 times more rapidly (and were not prevented by inertial forces from doing so) they would soon stop because of muscle fatigue, due mainly to potassium-induced membrane depolarization [59]. It follows that a mouse TA muscle with the same membrane properties as human TA would fatigue very rapidly (as described in the α2-pump knock-out mouse [47]), due to potassium accumulation in the t-tubules. Muscle membrane properties must therefore be different in smaller animals, to allow their limbs to move more rapidly [57].

BMR scales with surface area or mass$^{2/3}$, so that for a 1000-fold difference in weight, BMR per unit mass is 10 times higher for the smaller animal [60]. The higher BMR per unit mass is associated with greater Na/K-ATPase activity required to maintain transmembrane gradients, since smaller animals have leakier membranes due to a higher content of polyunsaturated phospholipids [58,61]. Leakier sarcolemma may also contribute to the reduced depolarizing afterpotential and early supernormality seen in mouse MVRCs (Fig. 2).

One limitation of this study is that we were not able to record *in vivo* from a slow-twitch predominantly oxidative mouse muscle. Mice have a far higher proportion of fast twitch glycolytic fibres than humans and they also have myosin heavy chain isoform type IIb fibres which are not present in human muscle [62]. Soleus is one of the few oxidative mouse muscles and has no type IIb fibres [62]. However, as soleus lies deep to the gastrocnemius and does not induce a specific, easily identifiable movement on contraction, it was impossible to be certain that we were recording from soleus *in vivo*. Determining the contribution of differences in fibre-type to species difference in MVRC profile will be a priority for future work. This is particularly important given the reported differences in ClC-1 conductance, Na_v expression and resting membrane potential between fast and slow-twitch muscle fibres [63].

4.4. Relevance to mice as models of neuromuscular disease

Our demonstration of marked differences in muscle excitability properties between mice and humans provides some insight into the phenotype differences between mice and humans with skeletal muscle channelopathies [12–14,64,65], and perhaps also other mouse models of neuromuscular disease [2,53,66,67].

The association of recessive myotonia congenita in mice, but not humans, with reduced body weight, muscle atrophy and a reduced life span [12] is in keeping with larger total and relative ClC-1 conductance in mouse skeletal muscle, as indicated by our findings with 9-anthracene carboxylic acid. Reduced ability of ClC-1 knockout animals to counter the effect of potassium accumulation likely provides a large metabolic burden on the mice by increasing reliance on energy-dependant α2-pump activity to maintain t-tubule potassium homoeostasis. A similar reduction in lifespan has not been reported for transgenic mouse models with myotonia secondary to mutation in $Na_V1.4$ [64,65] but male Draggen mice with $Na_V1.4$ myotonia do show higher energy expenditure and reduced total fat mass compared to their wild-type siblings [64]. There was no sex difference reported for transgenic mouse models of MC – both male and female adr mice exhibit reduced body weight and life span [12].

It was the observation of phenotype difference and relative resistance to PP attacks that initially inspired this work. This study does not allow us to comment definitively on the mechanism of resistance to spontaneous attacks in PP mice. However, the inferred greater activity of the α2-pump in mice is particularly interesting given that selective block of isolated muscle from mice with the $Na_V1.4$ R669H mutation for Hypokalaemic PP with 1 μM ouabain resulted in loss of force in baseline conditions, prevented recovery of force following exposure to hypokalaemia and lowered the threshold for hypokalaemia-induced weakness to occur [14]. Understanding the precise mechanisms involved in the apparent resistance of rodents to PP requires further work but is, we believe worth pursuing, as it should improve translation of studies using transgenic mice as a model of PP and may even highlight novel therapeutic options for PP patients.

MVRCs will be an effective tool for studying alterations to muscle physiology caused by a wide variety of muscle disorders, since membrane excitability properties are altered not just in conditions directly affecting muscle ion channels, but also as a consequence of pathology affecting muscle metabolism/energy supply, protein kinases and other interlinked processes [22–24,68–71]. The fact that MVRCs can be performed in both mice and humans with the same condition should facilitate effective translation of findings from mouse models to human subjects. In addition, where

a defined effect on skeletal muscle excitability is present, MVRCs may serve as a useful biomarker for trials of drugs / interventions for treatment of neuromuscular disorders.

Conclusion

In summary, we demonstrate significant differences in mouse and human skeletal muscle excitability. Our data proposes that in mouse muscle, (relatively) higher functional expression of the ClC-1 chloride channel and α2-pump contribute to reduced sensitivity to activity-dependant t-tubule potassium accumulation. This is likely an adaptation to a higher rate of muscle contraction in small animals. Our findings provide initial insights into the differences between mouse and human muscle physiology. A better understanding of these differences will enable more robust translation of data obtained from studies of mouse models of human neuromuscular disease. MVRCs are a valuable new tool that enables comparison of muscle membrane properties between species and will allow further characterisation of the molecular mechanisms regulating muscle excitability *in vivo*.

Declaration of Competing Interest

H. Bostock receives royalties from UCL for sales of his Qtrac software used in this study. The other authors have no conflicts of interest to disclose. All authors have approved the final paper.

Acknowledgements

We would like to thank Professor Thomas Pedersen from Aarhus, Denmark for helpful discussion of the manuscript. KS was supported by an MRC Clinical Research Training Fellowship (MR/M01827X/1) and is now an NIHR Clinical Lecturer in Clinical Neurophysiology. EM is supported by a Wellcome Trust Clinical Research Career Development Fellowship (209583/Z/17/Z). For the purpose of open access, the author has applied a CC BY public copyright licence to any Author Accepted Manuscript version arising from this submission. RM is supported by MRC grant MR/M006948/1. LG is The Graham Watts Senior Research Fellow and is supported by Brain Research UK. MGH work is supported by an MRC Centre grant and by the UCLH NIHR Biomedical Research Centre.

References

[1] Barré-Sinoussi F, Montagutelli X. Animal models are essential to biological research: issues and perspectives. Fut Sci OA 2015;1. doi:10.4155/fso.15.63.

[2] Perlman RL. Mouse models of human disease: an evolutionary perspective. Evol Med Public Health 2016;2016:170–6. doi:10.1093/emph/eow014.

[3] Wells D. Improving translational studies: lessons from rare neuromuscular diseases. Dis Model Mech 2015;8:1175–7. doi:10.1242/dmm.022616.

[4] Suetterlin K, Männikkö R, Hanna MG. Muscle channelopathies: recent advances in genetics, pathophysiology and therapy. Curr Opin Neurol 2014;27:583–90. doi:10.1097/WCO.0000000000000127.

[5] Zaharieva IT, Thor MG, Oates EC, van Karnebeek C, Hendson G, Blom E, et al. Loss-of-function mutations in SCN4A cause severe foetal hypokinesia or 'classical' congenital myopathy. Brain 2016;139:674–91. doi:10.1093/brain/awv352.

[6] Schartner V, Romero NB, Donkervoort S, Treves S, Munot P, Pierson TM, et al. Dihydropyridine receptor (DHPR, CACNA1S) congenital myopathy. Acta Neuropathol (Berl) 2017;133:517–33. doi:10.1007/s00401-016-1656-8.

[7] Elia N, Palmio J, Castañeda MS, Shieh PB, Quinonez M, Suominen T, et al. Myasthenic congenital myopathy from recessive mutations at a single residue in NaV1.4. Neurology 2019;92:1405–15. doi:10.1212/WNL.0000000000007185.

[8] Habbout K, Poulin H, Rivier F, Giuliano S, Sternberg D, Fontaine B, et al. A recessive Nav1.4 mutation underlies congenital myasthenic syndrome with periodic paralysis. Neurology 2016;86:161–9. doi:10.1212/WNL.0000000000002264.

[9] Tsujino A, Maertens C, Ohno K, Shen X-M, Fukuda T, Harper CM, et al. Myasthenic syndrome caused by mutation of the SCN4A sodium channel. Proc Natl Acad Sci 2003;100:7377–82. doi:10.1073/pnas.1230273100.

[10] Arnold WD, Feldman DH, Ramirez S, He L, Kassar D, Quick A, et al. Defective fast inactivation recovery of Nav1.4 in congenital myasthenic syndrome. Ann Neurol 2015;77:840–50. doi:10.1002/ana.24389.

[11] Chen M, Niggeweg R, Iaizzo PA, Lehmann-Horn F, Jockusch H. Chloride conductance in mouse muscle is subject to post-transcriptional compensation of the functional Cl− channel 1 gene dosage. J Physiol 1997;504:75–81. doi:10.1111/j.1469-7793.1997.075bf.x.

[12] Watkins WJ, Watts DC. Biological features of the new A2G–adr mouse mutant with abnormal muscle function. Lab Anim 1984;18:1–6.

[13] Wu F, Mi W, Hernández-Ochoa EO, Burns DK, Fu Y, Gray HF, et al. A calcium channel mutant mouse model of hypokalemic periodic paralysis. J Clin Invest 2012;122:4580–91. doi:10.1172/JCI66091.

[14] Wu F, Mi W, Burns DK, Fu Y, Gray HF, Struyk AF, et al. A sodium channel knockin mutant (NaV1.4-R669H) mouse model of hypokalemic periodic paralysis. J Clin Invest 2011;121:4082–94. doi:10.1172/JCI57398.

[15] Rüdel R, Ricker K, Lehmann-Horn F. Transient weakness and altered membrane characteristic in recessive generalized myotonia (Becker). Muscle Nerve 1988;11:202–11. doi:10.1002/mus.880110303.

[16] Bilbrey GL, Herbin L, Carter NW, Knochel JP. Skeletal muscle resting membrane potential in potassium deficiency. J Clin Invest 1973;52:3011–18. doi:10.1172/JCI107499.

[17] Z'Graggen WJ, Bostock H. Velocity recovery cycles of human muscle action potentials and their sensitivity to ischemia. Muscle Nerve 2009;39:616–26. doi:10.1002/mus.21192.

[18] Bergmans J. The negative after potential of human muscle fibres. Arch Int Physiol Biochim 1971;79:175–93. doi:10.3109/13813457109085301.

[19] Mihelin M, Trontelj JV, Stålberg E. Muscle fiber recovery functions studied with double pulse stimulation. Muscle Nerve 1991;14:739–47. doi:10.1002/mus.880140808.

[20] Boërio D, Z'graggen WJ, Tan SV, Guetg A, Ackermann K, Bostock H. Muscle velocity recovery cycles: effects of repetitive stimulation on two muscles. Muscle Nerve 2012;46:102–11. doi:10.1002/mus.23267.

[21] Z'Graggen WJ, Troller R, Ackermann KA, Humm AM, Bostock H. Velocity recovery cycles of human muscle action potentials: repeatability and variability. Clin Neurophysiol 2011;122:2294–9. doi:10.1016/j.clinph.2011.04.010.

[22] Z'Graggen WJ, Aregger F, Farese S, Humm AM, Baumann C, Uehlinger DE, et al. Velocity recovery cycles of human muscle action potentials in chronic renal failure. Clin Neurophysiol 2010;121:874–81. doi:10.1016/j.clinph.2010.01.024.

[23] Tankisi A, Pedersen TH, Bostock H, Z'Graggen WJ, Larsen LH, Meldgaard M, et al. Early detection of evolving critical illness myopathy with muscle velocity recovery cycles. Clin Neurophysiol Off J Int Fed Clin Neurophysiol 2021;132:1347–57. doi:10.1016/j.clinph.2021.01.017.

[24] Z'Graggen WJ, Brander L, Tuchscherer D, Scheidegger O, Takala J, Bostock H. Muscle membrane dysfunction in critical illness myopathy assessed by velocity recovery cycles. Clin Neurophysiol 2011;122:834–41. doi:10.1016/j.clinph.2010.09.024.
[25] Tan SV, Z'Graggen WJ, Boërio D, Rayan DR, Norwood F, Ruddy D, et al. Chloride channels in myotonia congenita assessed by velocity recovery cycles. Muscle Nerve 2014;49:845–57. doi:10.1002/mus.24069.
[26] Tan SV, Z'Graggen WJ, Hanna MG, Bostock H. In vivo assessment of muscle membrane properties in the sodium channel myotonias. Muscle Nerve 2018;57:586–94. doi:10.1002/mus.25956.
[27] Tan SV, Z'Graggen WJ, Boërio D, Rayan DLR, Howard R, Hanna MG, et al. Membrane dysfunction in Andersen-Tawil syndrome assessed by velocity recovery cycles. Muscle Nerve 2012;46:193–203. doi:10.1002/mus.23293.
[28] Tan SV, Suetterlin K, Männikkö R, Matthews E, Hanna MG, Bostock H. In vivo assessment of interictal sarcolemmal membrane properties in hypokalaemic and hyperkalaemic periodic paralysis. Clin Neurophysiol 2020;131:816–27. doi:10.1016/j.clinph.2019.12.414.
[29] Suetterlin KJ, Tan SV, Mannikko R, Phadke R, Orford M, Eaton S, et al. Ageing contributes to phenotype transition in a mouse model of periodic paralysis. JCSM Rapid Commun 2021;4:245–59. doi:10.1002/rco2.41.
[30] Tan SV, Z'Graggen WJ, Hanna MG, Bostock H. In vivo assessment of muscle membrane properties in the sodium channel myotonias. Muscle Nerve 2017:1–9. doi:10.1002/mus.25956.
[31] Pelosi L, Stevenson M, Hobbs GJ, Jardine A, Webb JK. Intraoperative motor evoked potentials to transcranial electrical stimulation during two anaesthetic regimens. Clin Neurophysiol 2001;112:1076–87. doi:10.1016/S1388-2457(01)00529-6.
[32] Boërio D, Greensmith L, Bostock H. A model of mouse motor nerve excitability and the effects of polarizing currents. J Peripher Nerv Syst 2011;16:322–33. doi:10.1111/j.1529-8027.2011.00364.x.
[33] Burke D, Bartley K, Woodforth IJ, Yakoubi A, Stephen JPH. The effects of a volatile anaesthetic on the excitability of human corticospinal axons. Brain 2000;123:992–1000. doi:10.1093/brain/123.5.992.
[34] Desaphy J-F, Costanza T, Carbonara R, Conte Camerino D. In vivo evaluation of antimyotonic efficacy of β-adrenergic drugs in a rat model of myotonia. Neuropharmacology 2013;65:21–7. doi:10.1016/j.neuropharm.2012.09.006.
[35] Ackermann KA, Bostock H, Brander L, Schröder R, Djafarzadeh S, Tuchscherer D, et al. Early changes of muscle membrane properties in porcine faecal peritonitis. Crit Care 2014;18:484. doi:10.1186/s13054-014-0484-2.
[36] Boërio D, Corrêa TD, Jakob SM, Ackermann KA, Bostock H, Z'Graggen WJ. Muscle membrane properties in A pig sepsis model: effect of norepinephrine. Muscle Nerve 2018;57:808–13. doi:10.1002/mus.26013.
[37] Frank GB. Negative after-potential of frog's skeletal muscle. J Neurophysiol 1957;20:602–14. doi:10.1152/jn.1957.20.6.602.
[38] Stalberg E. Propagation velocity in human muscle fibers in situ. Acta Physiol Scand Suppl 1966;287:1–112.
[39] Freygang WH, Goldstein DA, Hellam DC. The after-potential that follows trains of impulses in frog muscle fibers. J Gen Physiol 1964;47:929–52.
[40] Hino N. Some properties of late after-potential in frog skeletal muscle fiber. Jpn J Physiol 1977;27:235–50.
[41] Kirsch GE, Nichols RA, Nakajima S. Delayed rectification in the transverse tubules: origin of the late after-potential in frog skeletal muscle. J Gen Physiol 1977;70:1–21. doi:10.1085/jgp.70.1.1.
[42] Dutka TL, Murphy RM, Stephenson DG, Lamb GD. Chloride conductance in the transverse tubular system of rat skeletal muscle fibres: importance in excitation-contraction coupling and fatigue: t-system chloride conductance. J Physiol 2008;586:875–87. doi:10.1113/jphysiol.2007.144667.
[43] Pedersen T, de Paoli F, Flatman J. Regulation of ClC-1 and KATP channels in action potential–firing fast-twitch muscle fibers. J Gen 2009.
[44] Riisager A, de Paoli FV, Yu W-P, Pedersen TH, Chen T-Y, Nielsen OB. Protein kinase C-dependent regulation of ClC-1 channels in active human muscle and its effect on fast and slow gating. J Physiol 2016;594:3391–406. doi:10.1113/JP271556.
[45] DiFranco M, Yu C, Quiñonez M, Vergara JL. Inward rectifier potassium currents in mammalian skeletal muscle fibres. J Physiol 2015;593:1213–38. doi:10.1113/jphysiol.2014.283648.
[46] DiFranco M, Hakimjavadi H, Lingrel JB, Heiny JA. Na,K-ATPase α2 activity in mammalian skeletal muscle T-tubules is acutely stimulated by extracellular K+. J Gen Physiol 2015;146:281–94. doi:10.1085/jgp.201511407.
[47] Radzyukevich TL, Neumann JC, Rindler TN, Oshiro N, Goldhamer DJ, Lingrel JB, et al. Tissue-specific Role of the Na,K-ATPase α2 Isozyme in Skeletal Muscle. J Biol Chem 2013;288:1226–37. doi:10.1074/jbc.M112.424663.
[48] Hegarty PV, Hooper a C. Sarcomere length and fibre diameter distributions in four different mouse skeletal muscles. J Anat 1971;110:249–57.
[49] Maganaris CN. Force-length characteristics of in vivo human skeletal muscle. Acta Physiol Scand 2001;172:279–85. doi:10.1046/j.1365-201x.2001.00799.x.
[50] Mobley CB, Vechetti IJ, Valentino TR, McCarthy JJ. CORP: using transgenic mice to study skeletal muscle physiology. J Appl Physiol 2020;128:1227–39. doi:10.1152/japplphysiol.00021.2020.
[51] Webster RG. Animal models of the neuromuscular junction, vitally informative for understanding function and the molecular mechanisms of congenital myasthenic syndromes. Int J Mol Sci 2018;19. doi:10.3390/ijms19051326.
[52] Benatar M. Lost in translation: treatment trials in the SOD1 mouse and in human ALS. Neurobiol Dis 2007;26:1–13. doi:10.1016/j.nbd.2006.12.015.
[53] Elsea SH, Lucas RE. The mousetrap: what we can learn when the mouse model does not mimic the human disease. ILAR J 2002;43:66–79. doi:10.1093/ilar.43.2.66.
[54] Hu X, Charles JP, Akay T, Hutchinson JR, Blemker SS. Are mice good models for human neuromuscular disease? Comparing muscle excursions in walking between mice and humans. Skelet Muscle 2017;7:26. doi:10.1186/s13395-017-0143-9.
[55] Pearlman JP, Fielding RA. Creatine monohydrate as a therapeutic aid in muscular dystrophy. Nutr Rev 2006;64:80–8.
[56] Heglund NC, Taylor CR, McMahon TA. Scaling stride frequency. Science 1974;186:1112–13.
[57] Hill AV. The dimensions of animals and their muscular dynamics. Sci Prog 1950;38:209–30. doi:10.1111/j.1469-7998.2011.00830.x. Only.
[58] Hulbert AJ. Membranes and the setting of energy demand. J Exp Biol 2005;208:1593–9. doi:10.1242/jeb.01482.
[59] Lindinger MI, Cairns SP. Regulation of muscle potassium: exercise performance, fatigue and health implications. Eur J Appl Physiol 2021;121:721–48. doi:10.1007/s00421-020-04546-8.
[60] White CR, Seymour RS. Mammalian basal metabolic rate is proportional to body mass2/3. Proc Natl Acad Sci 2003;100:4046–9. doi:10.1073/pnas.0436428100.
[61] Wu BJ, Hulbert AJ, Storlien LH, Else PL. Membrane lipids and sodium pumps of cattle and crocodiles: an experimental test of the membrane pacemaker theory of metabolism. Am J Physiol Regul Integr Comp Physiol 2004;287:R633–41. doi:10.1152/ajpregu.00549.2003.
[62] Augusto V, Padovani CR, Campos GER. Skeletal muscle fiber types in C57BL6J mice. Braz J Morphol Sci 2004;21:89–94.
[63] Schiaffino S, Reggiani C. Fiber types in mammalian skeletal muscles. Physiol Rev 2011;91:1447–531. doi:10.1152/physrev.00031.2010.
[64] Corrochano S, Männikkö R, Joyce PI, McGoldrick P, Wettstein J, Lassi G, et al. Novel mutations in human and mouse SCN4A implicate AMPK in myotonia and periodic paralysis. Brain 2014;137:3171–85. doi:10.1093/brain/awu292.
[65] Hayward LJ, Kim JS, Lee M-Y, Zhou H, Kim JW, Misra K, et al. Targeted mutation of mouse skeletal muscle sodium channel produces myotonia and potassium-sensitive weakness. J Clin Invest 2008;118:1437–49. doi:10.1172/JCI32638.

[66] Phaneuf D, Wakamatsu N, Huang J-Q, Borowski A, Peterson AC, Fortunato SR, et al. Dramatically different phenotypes in mouse models of human Tay-Sachs and Sandhoff diseases. Hum Mol Genet 1996;5:1–14. doi:10.1093/hmg/5.1.1.

[67] Boërio D, Kalmar B, Greensmith L, Bostock H. Excitability properties of mouse motor axons in the mutant SOD1(G93A) model of amyotrophic lateral sclerosis. Muscle Nerve 2010;41:774–84. doi:10.1002/mus.21579.

[68] Call JA, Warren GL, Verma M, Lowe DA. Acute failure of action potential conduction in mdx muscle reveals new mechanism of contraction-induced force loss. J Physiol 2013;591:3765–76. doi:10.1113/jphysiol.2013.254656.

[69] Hirn C, Shapovalov G, Petermann O, Roulet E, Ruegg UT. Nav1.4 deregulation in dystrophic skeletal muscle leads to Na+ overload and enhanced cell death. J Gen Physiol 2008;132:199–208. doi:10.1085/jgp.200810024.

[70] Lee JH, Boland-Freitas R, Liang C, Ng K. Sarcolemmal depolarization in sporadic inclusion body myositis assessed with muscle velocity recovery cycles. Clin Neurophysiol 2019;130:2272–81. doi:10.1016/j.clinph.2019.08.019.

[71] Humm AM, Bostock H, Troller R, Z'Graggen WJ. Muscle ischaemia in patients with orthostatic hypotension assessed by velocity recovery cycles. J Neurol Neurosurg Psychiatry 2011;82:1394–8. doi:10.1136/jnnp-2011-300444.